IOPscience iopscience.iop.org

Home Search Collections Journals About Contact us My IOPscience

Evolution of averaged action variables in weakly non-integrable Hamiltonian systems

This article has been downloaded from IOPscience. Please scroll down to see the full text article.

2001 J. Phys. A: Math. Gen. 34 4999

(http://iopscience.iop.org/0305-4470/34/23/315)

View the table of contents for this issue, or go to the journal homepage for more

Download details:
IP Address: 171.66.16.95
The article was downloaded on 02/06/2010 at 09:00

Please note that terms and conditions apply.

INSTITUTE OF PHYSICS PUBLISHING JOURNAL OF PHYSICS A: MATHEMATICAL AND GENERAL

J. Phys. A: Math. Gen. **34** (2001) 4999–5019 www.iop.org/Journals/ja PII: S0305-4470(01)13605-X

# Evolution of averaged action variables in weakly non-integrable Hamiltonian systems

**Demin Yao and Jicong Shi**

Department of Physics and Astronomy, The University of Kansas, Lawrence, KS 66045, USA

Received 27 April 2000, in final form 26 February 2001

**Abstract**

The angle-averaged distribution function of action variables is studied by means of projection operators on the basis of the Liouville equation for the single-particle phase-space distribution of weakly non-integrable Hamiltonian systems. It is shown that the angle-averaged distribution function is governed by a kinetic equation similar to the Fokker–Planck equation but with a memory integral. An explicit form of the memory kernel is derived by a second-order perturbation expansion using the adiabatic and averaging approximations. For localized nonlinear perturbations, the kinetic equation takes the form of a functional map which can further be reduced to a moment map by using the Gaussian approximation. To examine the validity of this treatment, the evolution of actions is studied with examples of non-integrable systems. It is found that the result from the moment map agrees very well with the results from multi-particle tracking.

PACS numbers: 29.27.-a, 05.45.+b, 29.20.-c, 41.85.-p

## 1. Introduction

Diffusive motions in Hamiltonian systems are important to the understanding of many physical phenomena occurring in fluid dynamics, celestial mechanics, accelerators and other fields. Of the general Hamiltonian systems two limiting cases can be treated somewhat easily: strongly chaotic systems [1–3] and integrable systems in the presence of weak external noise [4,5]. In the former case, chaotic trajectories with their ergodic and short-memory-correlation properties enable a satisfactory description of the diffusion effect. In the latter, the delta-correlated external noise induces motions diffusing between KAM tori. Most real systems, however, are in the intermediate situations which are difficult to analyse because of the presence of both regular structures and chaotic regions. Another collective phenomenon that appears like diffusion is the transport of the phase space occupied by a distribution of particles. If the initial distribution does not match the KAM tori, filamentation of the phase-space region occupied by the particles will occur and it will result in an increase in the effective phase-space volume. In this paper we will consider the dynamical evolution of the phase-space particle distribution

0305-4470/01/234999+21$30.00 © 2001 IOP Publishing Ltd Printed in the UK 

with weakly non-integrable Hamiltonian models from beam dynamics in hadron accelerators or storage rings.

Generally, the dynamical behaviour of a weakly non-integrable Hamiltonian system such as hadron beam particles in an accelerator is characterized by two significantly different timescales in terms of action–angle variables. The angle variables vary quickly due to linear oscillations while the action variables change slowly due to nonlinear perturbations. The slow variation of the action variables contains all the information of the beam-size growth in accelerators. It is therefore possible to simplify the problem by averaging the angle variables over the short timescale. Such method of averaging provides a foundation for studying the mechanism of the beam-size growth perturbatively. Based on the perturbation theory with multiple scales, a perturbation expansion for the particle distribution in hadron storage rings has been developed recently to study the evolution of the beam size in phase space [6]. With this multiple-scale expansion, the equation of the distribution function becomes only action dependent. For localized nonlinear perturbations such as the beam–beam interaction at colliding points, this perturbation scheme results in a functional mapping for the particle distribution and the diffusion processes of particles in the beam can be studied numerically without resorting to the tracking of individual particles. Even though the multiple-scale expansion correctly described the physics of systems when only a few low-order resonances are dominant, it is very difficulty to consider high-order effects. In a previous paper [7] we have formulated a projection operator method (in its primitive form) for the study of the angle-averaged distribution function of the action variables only. This method was tested in systems with one and a half degrees of freedom and was found to be effective when long-time behaviour of the correlation functions of the motion becomes important [7]. In this paper, the projection operator method is elaborated in more detail in order to make a systematic second-order perturbation expansion for the relevant memory kernel which was approximated by its zeroth-order contribution in the previous paper. The second-order approach is found to be important for obtaining the proper long-time behaviour when more complicated systems, such as those of higher degrees of freedom, are considered. It should be noted that the projection operator method and the averaging technique have been used extensively in statistical physics [8]. The statistical approach of Hamiltonian beam dynamics has also been studied by Tzenov [9]. But his technique was limited to linear (integrable) systems. More recently, Channell introduced an averaging technique based on the canonical perturbation theory for studying the Vlasov equation when the non-integrable Hamiltonian is rapidly oscillating [10]. With this technique, the original Vlasov equation can be reduced to a Vlasov equation in 'slow' variables after averaging over the fast oscillation. Even though this approach can in principle apply to cases of nonlinear time evolution, it is still very difficult, if not impossible, to solve this Vlasov equation in 'slow' variables for non-integrable or near-integrable systems. One application of this Vlasov equation in 'slow' variables is the linear stability analysis of the stationary states of the distribution function [10]. For nonlinear multi-particle Hamiltonian systems, however, due to the lack of dissipation the particle distribution may not be able to reach any stationary state within the timescale under consideration. It is not even clear whether there are any stationary states for the nonlinear Vlasov equation. The time evolution (initial-value problem) of the particle distribution rather than the linear stability of stationary states is therefore important. It should also be noted that the averaging technique studied in this paper is used to eliminate the fast linear oscillations of angle variables while the averaging technique introduced by Channell [10] is primarily for the elimination of fast oscillation of external perturbations.

This paper is organized as follows. In section 2, the method of projection operator is introduced and applied to derive the evolution equation of the angle-averaged distribution function. In section 3, we discuss the approximation involved in order to obtain an explicit

computational formula. In section 4, the case of periodically kicked perturbations is discussed. A test of this method is carried out in section 5 by analysing examples of non-integrable systems. Section 6 contains conclusions and discussions.

## 2. Projection and the coarse-grained dynamics

In terms of action–angle variables $(\vec{I}, \vec{\phi}) \equiv (I_x, I_y, \phi_x, \phi_y)$, a weakly non-integrable Hamiltonian can be written as

$$H(\vec{I}, \vec{\phi}, t) = H_0(\vec{I}) + H_1(\vec{I}, \vec{\phi}, t) \tag{1}$$

where $H_0 = \vec{\nu}_0 \cdot \vec{I}$ is the integrable Hamiltonian and $H_1$ represents the non-integrable perturbation. For the particle motions in an accelerator, $H_0$ is the Hamiltonian for the linear betatron oscillation with betatron frequency $\vec{\nu}_0$, and $H_1$ is the Hamiltonian for the perturbation due to magnetic field errors, the beam–beam interaction, or space-charge force.

Consider a beam consisting of $N$ particles. If we neglect intra-beam collisions, the phase-space distribution of particles can be described by the single-particle distribution $f(\vec{I}, \vec{\phi}, t)$, which satisfies the Liouville equation

$$\frac{\partial f}{\partial t} = \hat{L}(t) f = \left[\hat{L}_0 + \hat{L}_1(t)\right] f \tag{2}$$

where

$$\hat{L}_0 f \equiv -\{H_0,\ f\} = -\vec{\nu}_0 \cdot \frac{\partial f}{\partial \vec{\phi}} \qquad \hat{L}_1 f \equiv -\{H_1,\ f\} \tag{3}$$

and $\{\cdot, \cdot\}$ denotes the Poisson bracket. In many cases, the small perturbation $H_1$ permits a perturbative treatment for equation (2). If the evolution of the distribution is known by solving equation (2), the averaged action variables that corresponds to the rms beam size can be evaluated from

$$\langle \vec{I} \rangle = \frac{1}{(2\pi)^2} \int \vec{I} f \, \mathrm{d}\vec{I} \, \mathrm{d}\vec{\phi} = \int \vec{I} \langle f \rangle_{\vec{\phi}} \, \mathrm{d}\vec{I} \tag{4}$$

where

$$\langle f \rangle_{\vec{\phi}} \equiv \frac{1}{(2\pi)^2} \int \mathrm{d}\vec{\phi}\ f(\vec{I}, \vec{\phi}, t) \tag{5}$$

denotes the angle-averaged distribution function. For the study of the beam-size growth, we thus need only this angle-averaged or reduced distribution function. The average of the angle variables can be conveniently described by introducing two projection operators orthogonal to each other:

$$\hat{P} f \equiv \langle f \rangle_{\vec{\phi}} \qquad \hat{Q} \equiv 1 - \hat{P}. \tag{6}$$

They satisfy $\hat{P}^2 = \hat{P}$, $\hat{Q}^2 = \hat{Q}$ and $\hat{P}\hat{Q} = \hat{Q}\hat{P} = 0$. It is not difficult to prove that

$$\hat{P}\hat{L}\hat{P} = 0 \qquad \hat{Q}\hat{L}_0 = \hat{L}_0\hat{Q} = \hat{L}_0 \qquad \hat{P}\hat{L}\hat{Q} = \hat{P}\hat{L}_1 \qquad \hat{Q}\hat{L}\hat{P} = \hat{L}_1\hat{P}. \tag{7}$$

To derive the equation of motion of the angle-averaged distribution function, we apply $\hat{P}$ and $\hat{Q}$ onto equation (2) and obtain [8]

$$\frac{\partial f_p}{\partial t} = \hat{P}\hat{L}\hat{P}\ f_p + \hat{P}\hat{L}\hat{Q}\ f_q \tag{8}$$

$$\frac{\partial f_q}{\partial t} = \hat{Q}\hat{L}\hat{P}\ f_p + \hat{Q}\hat{L}\hat{Q}\ f_q \tag{9}$$

where $f_p(\vec{I},t) \equiv \hat{P} f$ and $f_q(\vec{I},\vec{\phi},t) \equiv \hat{Q} f$. Assume that initially $f(\vec{I},\vec{\phi},0)$ is uniform in angle variables, i.e. $f_q(\vec{I},\vec{\phi},0) = 0$; $f_q$ can then be expressed in terms of $f_p$ as

$$f_q = \int_0^t \mathrm{d}t'\ \hat{U}_q(t,t')\hat{Q}\hat{L}(t')\hat{P}\ f_p(t') \tag{10}$$

where $\hat{U}_q(t,t')$ is the evolution operator (propagator) uniquely determined by

$$\frac{\partial \hat{U}_q(t,t')}{\partial t} = \hat{Q}\hat{L}(t)\hat{Q}\ \hat{U}_q(t,t') \qquad \hat{U}_q(t=t',t') = 1 \tag{11}$$

for arbitrary $t'$ and can be expressed in terms of a time-ordered exponential $\exp_T$ [8],

$$\hat{U}_q(t,t') = \exp_T\left\{\int_{t'}^t \mathrm{d}\tau\ \hat{Q}\hat{L}(\tau)\hat{Q}\right\} \tag{12}$$

which is understood as the Taylor expansion of the exponential with operators ordered from right to left as time increases. Substituting equation (10) into equation (8) results in a closed equation for $f_p$,

$$\frac{\partial f_p}{\partial t} = \hat{P}\hat{L}\hat{P}\ f_p + \int_0^t \mathrm{d}t'\ \hat{P}\hat{L}(t)\hat{Q}\,\hat{U}_q(t,t')\,\hat{Q}\hat{L}(t')\hat{P}\ f_p(t'). \tag{13}$$

Using equation (7), equation (13) is simplified to

$$\frac{\partial f_p}{\partial t} = \int_0^t \mathrm{d}t'\ \hat{P}\hat{L}_1(t)\hat{U}_q(t,t')\hat{L}_1(t')\hat{P}\ f_p(t'). \tag{14}$$

To derive a more explicit expression we make the following observations. First,

$$\hat{L}_1\hat{P} f_p = -\{H_1,\ f_p\} = \frac{\partial H_1}{\partial \vec{\phi}} \cdot \frac{\partial f_p}{\partial \vec{I}} \tag{15}$$

and, for an arbitrary function $g(\vec{I},\vec{\phi})$,

$$\hat{P}\hat{L}_1 g = \frac{\partial}{\partial \vec{I}} \cdot \left\langle \frac{\partial H_1}{\partial \vec{\phi}}\ g \right\rangle_{\vec{\phi}}. \tag{16}$$

Second, when $H_1 = 0$, $\hat{U}_q(t,t')$ is the unperturbed propagator,

$$\hat{U}_q(t,t') = \hat{U}_0(t-t') \equiv \exp[(t-t')\hat{L}_0] \tag{17}$$

and its action on an arbitrary function $g(\vec{I},\vec{\phi})$ is simply

$$\hat{U}_0(t)g(\vec{I},\vec{\phi}) = g\big(\vec{I},\hat{U}_0(t)\vec{\phi}\big) = g\big(\vec{I},\vec{\phi}-\vec{\nu}_0 t\big). \tag{18}$$

This prompts us to peel off the unperturbed contribution by introducing

$$\hat{U}_q(t,t') \equiv \hat{U}_{1q}(t,t')\hat{U}_0(t-t'). \tag{19}$$

It can be shown that

$$\hat{U}_{1q}(t,t') = \exp_T \int_{t'}^t \mathrm{d}\tau\ \hat{Q}\hat{L}_1'(\tau;t-\tau)\hat{Q} \tag{20}$$

where

$$\hat{L}_1'(t;t')\,g = \hat{U}_0(t')\hat{L}_1(t)\hat{U}_0^{-1}(t')\,g = -\{H_1(\vec{I},\vec{\phi}-\vec{\nu}_0 t',t),\ \ g\}. \tag{21}$$

Substituting equations (15), (16), (18), (19) into (14), we obtain the equation of the angle-averaged distribution function in a more explicit form:

$$\frac{\partial}{\partial t} f_p(\vec{I},t) = \int_0^t \mathrm{d}t' \sum_{i,j} \frac{\partial}{\partial I_i} D_{ij}(\vec{I},t,t') \frac{\partial}{\partial I_j} f_p(\vec{I},t') \tag{22}$$

where

$$D_{ij}(\vec{I},t,t') \equiv \left\langle \frac{\partial H_1(\vec{I},\vec{\phi},t)}{\partial \phi_i}\ \hat{U}_{1q}(t,t')\ \frac{\partial H_1(\vec{I},\vec{\phi}-\vec{v}_0(t-t'),t')}{\partial \phi_j} \right\rangle_{\vec{\phi}}. \tag{23}$$

Only the $Q$-projected perturbed propagator $\hat{U}_{1q}$ is still implicit. It should be noted that the appearance of the diffusion-like operators in terms of the action variables guarantees the conservation of probability

$$\frac{\mathrm{d}}{\mathrm{d}t}\int \mathrm{d}\vec{I}\ f_p(\vec{I},t) = 0 \tag{24}$$

and when $H_1$ does not depend on $\vec{\phi}$, $f_p$ itself does not change with time.

## 3. Adiabatic and averaging approximation

In order to solve equation (22) for $f_p$, the correlation functions $D_{ij}(\vec{I},t,t')$ defined in equation (23) have to be explicitly given. Further approximations are therefore needed to deal with $\hat{U}_{1q}$. Since $\hat{Q}\hat{P} = 0$, it follows that $\hat{U}_{1q}(t,t')\hat{P} = \hat{P}$, i.e. $\hat{U}_{1q}$ has no action on a function containing only action variables. On the other hand, for the problem of the slow beam-size growth, the action variables are adiabatic invariants during the timescale of the linear oscillation. It is therefore possible to approximate the action of $\hat{U}_{1q}$ by acting on the angle variables only. For instance, for any Fourier mode $g_{\vec{m}}(\vec{I})\exp(\mathrm{i}\vec{m}\cdot\vec{\phi})$ of an arbitrary function $g(\vec{I},\vec{\phi})$,

$$\hat{U}_{1q}(t,t')\left[g_{\vec{m}}(\vec{I})\exp(\mathrm{i}\vec{m}\cdot\vec{\phi})\right] \approx g_{\vec{m}}(\vec{I})\ \hat{U}_{1q}(t,t')\exp(\mathrm{i}\vec{m}\cdot\vec{\phi}). \tag{25}$$

To derive an explicit approximation formula we start from the expansion form of $\hat{U}_{1q}(t,t')$

$$\begin{aligned}\hat{U}_{1q}(t,t') = 1 &+ \int_{t'}^{t}\mathrm{d}\tau_1\ \hat{Q}\hat{L}_1'(\tau_1;t-\tau_1)\hat{Q} \\ &+ \int_{t'}^{t}\mathrm{d}\tau_1\int_{t'}^{\tau_1}\mathrm{d}\tau_2\ \hat{Q}\hat{L}_1'(\tau_1;t-\tau_1)\hat{Q}\hat{L}_1'(\tau_2;t-\tau_2)\hat{Q}+\cdots.\end{aligned} \tag{26}$$

The adiabatic approximation implies that we may neglect terms containing differentiations with respect to the action variables, i.e. for an arbitrary function $g(\vec{I},\vec{\phi})$,

$$\hat{Q}\hat{L}_1'(t_1;t_2)\hat{Q}\ g\ \approx -\hat{Q}\left\{\frac{\partial H_1(\vec{I},\vec{\phi},t_1)}{\partial \vec{I}}\cdot\frac{\partial g}{\partial \vec{\phi}}\right\} \tag{27}$$

$$\begin{aligned}\hat{Q}\hat{L}_1'(t_1;t_2)\hat{Q}\hat{L}_1'(t_3;t_4)\hat{Q}\ g \approx\ \hat{Q}\sum_{i,j}\Bigg\{&\left[\frac{\partial H_1(\vec{I},\vec{\phi}-\vec{v}_0t_2,t_1)}{\partial I_j}\ \frac{\partial^2 H_1(\vec{I},\vec{\phi}-\vec{v}_0t_4,t_3)}{\partial\phi_j\partial I_i}\right. \\ &\left.-\frac{\partial H_1(\vec{I},\vec{\phi}-\vec{v}_0t_2,t_1)}{\partial\phi_j}\ \frac{\partial^2 H_1(\vec{I},\vec{\phi}-\vec{v}_0t_4,t_3)}{\partial I_j\partial I_i}\right]\frac{\partial g}{\partial\phi_i} \\ &+\frac{\partial H_1(\vec{I},\vec{\phi}-\vec{v}_0t_2,t_1)}{\partial I_j}\ \frac{\partial H_1(\vec{I},\vec{\phi}-\vec{v}_0t_4,t_3)}{\partial I_i}\ \frac{\partial^2 g}{\partial\phi_j\partial\phi_i} \\ &+\frac{\partial H_1(\vec{I},\vec{\phi}-\vec{v}_0t_2,t_1)}{\partial\phi_j}\left\langle\frac{\partial^2 H_1(\vec{I},\vec{\phi}-\vec{v}_0t_4,t_3)}{\partial I_j\partial I_i}\frac{\partial g}{\partial\phi_i}\right\rangle_{\vec{\phi}}\Bigg\}.\end{aligned} \tag{28}$$

We further make the following averaging approximation. Note that in equations (27) and (28) all coefficient functions associated with the differentiations to the angle variables of

$g(\vec{I},\vec{\phi})$ contain perturbing Hamiltonian $H_1$. Similar to the canonical transformation of non-integrable Hamiltonians, their angle averages or secular terms lead to a change of frequencies with amplitudes. The oscillatory terms contribute only to higher-order perturbations and can be neglected for sufficiently small nonlinearity. After neglecting all oscillatory terms in the coefficient functions, $\hat{Q}$ can be dropped and equations (27) and (28) become

$$\hat{Q}\hat{L}_1'(t_1;t_2)\hat{Q} \approx -\left\langle \frac{\partial H_1(\vec{I},\vec{\phi},t_1)}{\partial \vec{I}} \right\rangle_{\vec{\phi}} \cdot \frac{\partial}{\partial \vec{\phi}} \tag{29}$$

$$\begin{aligned}\hat{Q}\hat{L}_1'(t_1;t_2)\hat{Q}\hat{L}_1'(t_3;t_4)\hat{Q} \approx &-\sum_{i,j}\left[\frac{\partial}{\partial I_j}\left\langle \frac{\partial H_1'(\vec{I},\vec{\phi},t_1)}{\partial \phi_j}\frac{\partial H_1'(\vec{I},\vec{\phi}-\vec{\nu}_0(t_4-t_2),t_3)}{\partial I_i}\right\rangle_{\vec{\phi}}\right]\frac{\partial}{\partial \phi_i}\\ &+\sum_{i,j}\left\langle \frac{\partial H_1'(\vec{I},\vec{\phi},t_1)}{\partial I_j}\frac{\partial H_1'(\vec{I},\vec{\phi}-\vec{\nu}_0(t_4-t_2),t_3)}{\partial I_i}\right\rangle_{\vec{\phi}}\frac{\partial^2}{\partial \phi_j\partial \phi_i}\\ &+\sum_{i,j}\left\langle \frac{\partial H_1(\vec{I},\vec{\phi},t_1)}{\partial I_j}\right\rangle_{\vec{\phi}}\left\langle \frac{\partial H_1(\vec{I},\vec{\phi},t_3)}{\partial I_i}\right\rangle_{\vec{\phi}}\frac{\partial^2}{\partial \phi_j\partial \phi_i}\end{aligned} \tag{30}$$

where

$$H_1'(\vec{I},\vec{\phi},\tau) = H_1(\vec{I},\vec{\phi},\tau) - \left\langle H_1(\vec{I},\vec{\phi},\tau)\right\rangle_{\vec{\phi}}. \tag{31}$$

Finally, we rewrite $\hat{U}_{1q}(t,t')$ into exponential form and keep only up to the second-order contributions from $H_1$,

$$\hat{U}_{1q}(t,t') \approx \exp\left[\hat{L}_{\vec{\phi}}(t,t')\right] \tag{32}$$

with

$$\begin{aligned}\hat{L}_{\vec{\phi}}(t,t') = &-\sum_i \int_{t'}^{t} \mathrm{d}\tau_1 \left\langle \frac{\partial H_1(\vec{I},\vec{\phi},\tau_1)}{\partial I_i}\right\rangle_{\vec{\phi}}\frac{\partial}{\partial \phi_i} - \sum_{i,j}\int_{t'}^{t}\mathrm{d}\tau_1\\ &\times\int_{t'}^{\tau_1}\mathrm{d}\tau_2\left[\frac{\partial}{\partial I_j}\left\langle \frac{\partial H_1'(\vec{I},\vec{\phi},\tau_1)}{\partial \phi_j}\frac{\partial H_1'(\vec{I},\vec{\phi}-\vec{\nu}_0(\tau_1-\tau_2),\tau_2)}{\partial I_i}\right\rangle_{\vec{\phi}}\right]\frac{\partial}{\partial \phi_i}\\ &+\sum_{i,j}\int_{t'}^{t}\mathrm{d}\tau_1\int_{t'}^{\tau_1}\mathrm{d}\tau_2\left\langle \frac{\partial H_1'(\vec{I},\vec{\phi},\tau_1)}{\partial I_j}\frac{\partial H_1'(\vec{I},\vec{\phi}-\vec{\nu}_0(\tau_1-\tau_2),\tau_2)}{\partial I_i}\right\rangle_{\vec{\phi}}\frac{\partial^2}{\partial \phi_j\partial \phi_i}.\end{aligned} \tag{33}$$

It should be noted that the last term of equation (30) does not appear in equation (33) after rewriting $\hat{U}_{1q}(t,t')$ into exponential form. This can be seen if one compares the expansion in equation (26) and the expansion in equations (32) and (33). The latter expansion resembles a cumulant expansion, i.e. the exponent rather than the time-ordered exponential itself is expanded.

The diffusion coefficients given by equation (23) can then be calculated, using equation (32), by

$$D_{ij}(\vec{I},t,t') \approx \left\langle \frac{\partial H_1(\vec{I},\vec{\phi},t)}{\partial \phi_i}\ \exp\left[\hat{L}_{\vec{\phi}}(t,t')\right]\frac{\partial H_1(\vec{I},\vec{\phi}-\vec{\nu}_0(t-t'),t')}{\partial \phi_j}\right\rangle_{\vec{\phi}}. \tag{34}$$

Note that the first two terms of $\hat{L}_{\vec{\phi}}$ in equation (33) contribute to the first- and second-order amplitude dependence of the frequencies, respectively, while the third term of $\hat{L}_{\vec{\phi}}$ results in diffusion in angular space. In our previous paper [7], $\exp\left[\hat{L}_{\vec{\phi}}(t,t')\right]$ was approximated by its zeroth-order contribution which is simply an identity operator. The inclusion of high-order

contribution of $\hat{L}_{\vec{\phi}}$ was found to be important to the long-term behaviour of high-dimensional systems. For a more explicit expression of $D_{ij}$, we decompose $H_1$ into Fourier modes as

$$H_1 = \sum_{\vec{m}} h_{\vec{m}}(I,t)\exp\{\mathrm{i}\vec{m}\cdot\vec{\phi}\} \tag{35}$$

with $h_{-\vec{m}} = h^*_{\vec{m}}$ and obtain

$$\begin{aligned}\hat{L}_{\vec{\phi}}(t,t') = &-\sum_i \int_{t'}^{t} \mathrm{d}\tau_1 \, \frac{\partial h_{\vec{0}}(\vec{I},\tau_1)}{\partial I_i}\frac{\partial}{\partial \phi_i} - \sum_{\vec{m}\neq\vec{0}}\sum_{i,j}\int_{t'}^{t}\mathrm{d}\tau_1\int_{t'}^{\tau_1}\mathrm{d}\tau_2\ \exp[\mathrm{i}(\tau_1-\tau_2)\vec{m}\cdot\vec{\nu}_0] \\ &\times\left\{ im_j\left[\frac{\partial}{\partial I_j}\left(h_{\vec{m}}(\vec{I},\tau_1)\frac{\partial h^*_{\vec{m}}(\vec{I},\tau_2)}{\partial I_i}\right)\right]\frac{\partial}{\partial\phi_i}\right. \\ &\left. -\frac{\partial h_{\vec{m}}(\vec{I},\tau_1)}{\partial I_j}\frac{\partial h^*_{\vec{m}}(\vec{I},\tau_2)}{\partial I_i}\frac{\partial^2}{\partial\phi_j\partial\phi_i}\right\}.\end{aligned} \tag{36}$$

The diffusion coefficients can then be calculated from

$$D_{ij}(\vec{I},t,t') \approx \sum_{\vec{n}} n_i n_j\ h_{\vec{n}}(\vec{I},t)h^*_{\vec{n}}(\vec{I},t')\ \exp\left[\mathrm{i}\vec{n}\cdot\vec{\nu}_0(t-t') + E(\vec{n},t,t')\right] \tag{37}$$

where

$$\begin{aligned}E(\vec{n},t,t') = &\ \mathrm{i}\vec{n}\cdot\int_{t'}^{t}\mathrm{d}\tau_1\ \frac{\partial h_{\vec{0}}(\vec{I},\tau_1)}{\partial\vec{I}} \\ &-\vec{n}\cdot\sum_{\vec{m}\neq\vec{0}}\int_{t'}^{t}\mathrm{d}\tau_1\int_{t'}^{\tau_1}\mathrm{d}\tau_2\ \exp[\mathrm{i}(\tau_1-\tau_2)\vec{m}\cdot\vec{\nu}_0]\left(\vec{m}\cdot\frac{\partial}{\partial\vec{I}}\right) \\ &\times\left[h_{\vec{m}}(\vec{I},\tau_1)\frac{\partial h^*_{\vec{m}}(\vec{I},\tau_2)}{\partial\vec{I}}\right] \\ &-\frac{1}{2}\sum_{\vec{m}\neq\vec{0}}\left|\vec{n}\cdot\int_{t'}^{t}\mathrm{d}\tau_1\ \frac{\partial h_{\vec{m}}(\vec{I},\tau_1)}{\partial\vec{I}}\exp(\mathrm{i}\tau_1\vec{m}\cdot\vec{\nu}_0)\right|^2.\end{aligned} \tag{38}$$

Note that only Fourier components with $\vec{m} \neq \vec{0}$ are important for $D_{ij}$. It should be emphasized that the adiabatic approximation used in equations (27) and (28) and the averaging approximation used in equations (29) and (30) lead to an asymptotic expansion for $D_{ij}$ and the validity of these approximations needs to be tested with dynamics systems (see section 5).

## 4. Kick-type perturbations

For the particle motion in a high-energy accelerator, the nonlinear perturbation $H_1$ is usually from either beam–beam interactions at interaction points or localized magnetic-field errors in the ring. $H_1$ can therefore be represented by periodic kicks. Consider a periodic kick

$$H_1(\vec{I},\vec{\phi},t) = H_1(\vec{I},\vec{\phi})\ \delta_p(t) \qquad \delta_p(t) = \sum_{k=-\infty}^{\infty}\delta(t-2\pi k) \tag{39}$$

where, to simplify the notation, we have used $H_1(\vec{I},\vec{\phi})$ to denote the time-independent factor of $H_1(\vec{I},\vec{\phi},t)$, and $\delta(t-2\pi k)$ is the Dirac delta function which represents the kick occurring at $t = 2\pi k$. Let

$$F_n(\vec{I}) = f_p(\vec{I}, t = 2\pi n^-) \tag{40}$$

denote the angle-averaged distribution function after the beam has circulated $n$ revolutions but before passing the kick. Substituting equation (39) into (34) and integrating equation (22) yields

$$F_{n+1}(\vec{I}) = F_n(\vec{I}) + \frac{1}{2}\sum_{i,j}\frac{\partial}{\partial I_i}\left\langle\frac{\partial H_1}{\partial\phi_i}\frac{\partial H_1}{\partial\phi_j}\right\rangle_{\vec{\phi}}\frac{\partial}{\partial I_j}F_n(\vec{I}) + \sum_{m=0}^{n-1}\sum_{i,j}\frac{\partial}{\partial I_i}\left\langle\frac{\partial H_1}{\partial\phi_i}\ \exp\left[\hat{L}_{\vec{\phi}}(n-m)\right]\frac{\partial H_1^{(n-m)}}{\partial\phi_j^{(n-m)}}\right\rangle_{\vec{\phi}}\frac{\partial}{\partial I_j}F_m(\vec{I}) \tag{41}$$

where

$$\hat{L}_{\vec{\phi}}(k) = -k\sum_i\left\langle\frac{\partial H_1}{\partial I_i}\right\rangle_{\vec{\phi}}\frac{\partial}{\partial\phi_i} - \frac{1}{2}k\sum_{i,j}\left[\frac{\partial}{\partial I_j}\left\langle\frac{\partial H_1'}{\partial\phi_j}\frac{\partial H_1'}{\partial I_i}\right\rangle_{\vec{\phi}}\right]\frac{\partial}{\partial\phi_i} - \sum_{l=1}^{k-1}\sum_{i,j}(k-l)\left[\frac{\partial}{\partial I_j}\left\langle\frac{\partial H_1'}{\partial\phi_j}\frac{\partial H_1'^{(l)}}{\partial I_i}\right\rangle_{\vec{\phi}}\right]\frac{\partial}{\partial\phi_i} + \frac{1}{2}\sum_{l,l'=1}^{k}\sum_{i,j} \times\left\langle\frac{\partial H_1'^{(l)}}{\partial I_j}\frac{\partial H_1'^{(l')}}{\partial I_i}\right\rangle_{\vec{\phi}}\frac{\partial^2}{\partial\phi_j\partial\phi_i} \tag{42}$$

and

$$H_1^{(k)} = H_1(\vec{I},\vec{\phi}^{(k)}) \qquad H_1'^{(k)} = H_1^{(k)} - \langle H_1\rangle_{\vec{\phi}} \qquad \vec{\phi}^{(k)} = \hat{U}_0(2\pi k^-, 0^-)\vec{\phi}. \tag{43}$$

The numerical factor $1/2$ in front of the second term in the right-hand sides of equations (41) and (42) is due to the fact that an integral of a Dirac delta function which evaluates at the boundary of the integral equals $1/2$. Note that $\hat{U}_0(2\pi n^-, 2\pi m^-) = \hat{U}_0(2\pi(n-m)^-, 0^-)$ because of the periodicity.

Equation (41) is a functional mapping which provides a computational means for calculating the angle-averaged distribution. In terms of the Fourier components of $H_1(\vec{I},\vec{\phi})$ in equation (35), this functional mapping can further be written in a more explicit form as

$$F_{n+1}(\vec{I}) = F_n(\vec{I}) + \frac{1}{2}\sum_{\vec{m}}\left(\vec{m}\cdot\frac{\partial}{\partial\vec{I}}\right)\left|h_{\vec{m}}(\vec{I})\right|^2\left(\vec{m}\cdot\frac{\partial}{\partial\vec{I}}\right)F_n(\vec{I}) + \sum_{l=0}^{n-1}\sum_{\vec{m}}\left(\vec{m}\cdot\frac{\partial}{\partial\vec{I}}\right)\left\{\left|h_{\vec{m}}(\vec{I})\right|^2\cos[2\pi(n-l)\vec{m}\cdot\vec{\nu}]\right\}\left(\vec{m}\cdot\frac{\partial}{\partial\vec{I}}\right)F_l(\vec{I}) \tag{44}$$

where

$$\vec{\nu} = \vec{\nu}_0 + \Delta\vec{\nu} \qquad \Delta\vec{\nu} = \frac{1}{2\pi}\frac{\partial}{\partial\vec{I}}\left\{h_{\vec{0}}(\vec{I}) - \frac{1}{4}\sum_{\vec{m}\neq\vec{0}}\vec{m}\cdot\frac{\partial|h_{\vec{m}}|^2}{\partial\vec{I}}\cot(\pi\vec{m}\cdot\vec{\nu}_0)\right\}. \tag{45}$$

In deriving equation (44) we have retained only those contributions from $\hat{L}_{\vec{\phi}}(k)$ that are proportional to $k$ for large $k$, which are dominant for long-term behaviours. This results in the first- and second-order amplitude dependence of frequencies in equation (45). While the first-order amplitude dependence is determined solely by zero-mode Fourier component, the second-order amplitude dependence is the contribution from nonzero-mode Fourier components. Similar to the canonical perturbation expansion or normal-form expansion [11], the factor $\cot(\pi\vec{m}\cdot\vec{\nu}_0)$ in equation (45) reminds us to stay away from major resonances to prevent the perturbation results from breaking down. It should be noted that in our previous treatment [7] only the zeroth-order contribution of $\hat{L}_{\vec{\phi}}(k)$ was retained and the amplitude dependence of

frequencies was included into $H_0$. In the current approach, effects of the amplitude dependence of frequencies are automatically considered through $\hat{L}_{\vec{\phi}}(k)$.

As mentioned before, our main concern is the beam-size growth characterized by the first-order moments of the angle-averaged distribution function

$$\vec{M}_n = \int \mathrm{d}\vec{I}\ \vec{I} F_n(\vec{I}) \tag{46}$$

Naturally, we are motivated to derive the mapping equations for $\vec{M}_n$. Such equations, however, involve the higher-order moments due to the nonlinearity of the system and, therefore, truncations must be made to obtain the closure. On the other hand, experimental observations have shown that the particle distribution in large particle storage rings remains approximately Gaussian if it is initially a Gaussian distribution. As the beam circulates in the ring, the distribution is gradually distorted with a growth of the distribution tail. In this case, we may further simplify the functional mapping (44) by using a Gaussian distribution approximation in which $F_n(\vec{I})$ is approximated by a Gaussian distribution [6]

$$F_n(\vec{I}) \approx G(\vec{M}_n, \vec{I}) = \frac{1}{M_{xn} M_{yn}} \exp\left(-\frac{I_x}{M_{xn}} - \frac{I_y}{M_{yn}}\right) \tag{47}$$

and then integrate the functional mapping (44) multiplied by $\vec{I}$. A two-dimensional nonlinear mapping for $\vec{M}_n$ is thus obtained as

$$\begin{aligned}\vec{M}_{n+1} = \vec{M}_n &- \frac{1}{2}\sum_{\vec{m}} \vec{m} \int \mathrm{d}\vec{I}\ \left|h_{\vec{m}}(\vec{I})\right|^2 \left[\vec{m}\cdot\frac{\partial}{\partial \vec{I}} G(\vec{M}_n, \vec{I})\right] \\ &- \sum_{l=0}^{n-1}\sum_{\vec{m}} \vec{m} \int \mathrm{d}\vec{I}\ \left|h_{\vec{m}}(\vec{I})\right|^2 \cos[2\pi(n-l)\vec{m}\cdot\vec{\nu}] \left[\vec{m}\cdot\frac{\partial}{\partial \vec{I}} G(\vec{M}_l, \vec{I})\right].\end{aligned} \tag{48}$$

It should be noted that the approximation in equation (47) may not be appropriate for representing the distribution function as a whole even when it is good for analysing the evolution of the first-order moments.

## 5. Examples

To test the method of projection operator for the angle-averaged distribution function, the evolution of average actions is studied on examples of two- and four-dimensional symplectic maps. The average actions calculated with the angle-averaged distribution function is compared with the result of numerical simulations of the distribution function. The first example of the two-dimensional map was studied in our previous paper [7] where only the first-order contribution to the amplitude dependence of frequency was considered. To examine the current approach that includes the second-order contribution, this example is studied here again.

(1) Non-integrable system with one and a half degrees of freedom. Consider a two-dimensional symplectic map

$$\begin{aligned} x_{n+1} &= x_n \cos 2\pi\nu_0 + [p_n + K(x_n)] \sin 2\pi\nu_0 \\ p_{n+1} &= -x_n \sin 2\pi\nu_0 + [p_n + K(x_n)] \cos 2\pi\nu_0 \end{aligned} \tag{49}$$

where $\nu_0$ is the frequency for the linear rotation. The nonlinear kick force can be expanded as $K(x) = \sum_{m=2} \epsilon_{m-1} x^m$, where $\epsilon_{m-1}$ is the strength of the $m$th-order multipole. Map (49) describes the horizontal motion of beam particles in a hadron storage ring. As an example,

we consider sextupole and octupole only, i.e. $K(x) = \epsilon_1 x^2 + \epsilon_2 x^3$, and the corresponding Hamiltonian is

$$H_0 = \nu_0 I \qquad \text{and} \qquad H_1 = -\left[\frac{\epsilon_1}{3}(2I)^{3/2}\cos^3\phi + \frac{\epsilon_2}{4}(2I)^2\cos^4\phi\right]\delta_p(t) \tag{50}$$

where the action–angle variables are related to the Cartesian phase-space coordinates by $x = \sqrt{2I}\cos\phi$, $p = -\sqrt{2I}\sin\phi$. Substituting this Hamiltonian into equation (44) yields

$$\begin{aligned} F_{n+1}(I) = F_n(I) &+ \frac{1}{4}\frac{\mathrm{d}}{\mathrm{d}I}\left(\epsilon_1^2 I^3 + \frac{5\epsilon_2^2}{4} I^4\right)\frac{\mathrm{d}}{\mathrm{d}I}F_n(I) \\ &+ \frac{1}{4}\sum_{m=1}^{n}\frac{\mathrm{d}}{\mathrm{d}I}\left\{\epsilon_1^2\left[\cos(2\pi m\nu) + \cos(6\pi m\nu)\right] I^3\right. \\ &\left. + \frac{\epsilon_2^2}{2}\left[4\cos(4\pi m\nu) + \cos(8\pi m\nu)\right] I^4\right\}\frac{\mathrm{d}}{\mathrm{d}I}F_{n-m}(I) \end{aligned} \tag{51}$$

where the frequency $\nu$ is calculated from equation (45) as

$$\nu = \nu_0 + \frac{\epsilon_1^2\lambda}{2\pi} I \qquad \lambda = -\tfrac{1}{8}\{6\alpha + [3\cot(\pi\nu_0) + \cot(3\pi\nu_0)]\} \tag{52}$$

with $\alpha = \epsilon_2/\epsilon_1^2$. For the amplitude dependence of frequency $\nu$, we include only the lowest-order term, linear amplitude dependence, which is the first-order contribution from octupole and the second-order contribution from sextupole. The nonlinear mapping for the moment is obtained from equation (48) as

$$\begin{aligned} \sigma_{n+1} = \sigma_n &+ \tfrac{3}{2}\left[\sigma_n^2 + 5\alpha^2\sigma_n^3\right] \\ &+ \tfrac{3}{2}\sum_{m=1}^{n}\left\{\sigma_{n-m}^2\left[R_1(2\pi m\nu_0, m\lambda\sigma_{n-m}) + R_1(6\pi m\nu_0, 3m\lambda\sigma_{n-m})\right]\right. \\ &\left. + 2\alpha^2\sigma_{n-m}^3\left[4\,R_2(4\pi m\nu_0, 2m\lambda\sigma_{n-m}) + R_2(8\pi m\nu_0, 4m\lambda\sigma_{n-m})\right]\right\} \end{aligned} \tag{53}$$

where $\sigma_n = \epsilon_1^2 M_{xn}$ is the average action scaled with $\epsilon_1^2$ that represents rms beam size in phase space and

$$R_1(x, y) = \frac{1}{(1+y^2)^4}\left[(1 - 6y^2 + y^4)\,\cos x - 4y(1 - y^2)\,\sin x\right] \tag{54}$$

$$R_2(x, y) = \frac{1}{(1+y^2)^5}\left[(1 - 10y^2 + 5y^4)\,\cos x - y(5 - 10y^2 + y^4)\,\sin x\right]. \tag{55}$$

Note that the moment map (53) contains only three parameters: $\nu_0$, the initial moment $\sigma_0$ and the ratio of octupole and sextupole strength $\alpha$. Numerical calculations of the time evolution of the moment have been carried out by using the moment map and, to test the results, by the multi-particle tracking for direct simulation of the moment.

Figure 1 plots the evolution of the average action for the example of $\nu_0 = 0.2114$ and $\alpha = 0$. In this case, map (48) is a two-dimensional Hénon map. A comparison between the result of the moment map (53) and the result of the direct tracking shows a good agreement between the two methods. When $\sigma_0$ is small as compared with the dynamic aperture (the stable boundary for single-particle dynamics), there is always a stationary state for the average action after transient oscillations die out. For small $\sigma_0$, particles of beam stay inside the dynamic aperture where the phase space is foliated by KAM tori and resonances. The existence of stationary state for the average action is therefore due to the presence of KAM tori. Note that the dynamic aperture in this case is at $I = (x^2 + p^2)/2 \simeq 0.08$. The transient oscillation, on the other hand, is due to angular rotation arising from $H_0$ and has a quasi-period of $1/\nu_0$. Since the approximations involved for obtaining the moment map are for the elimination of angular

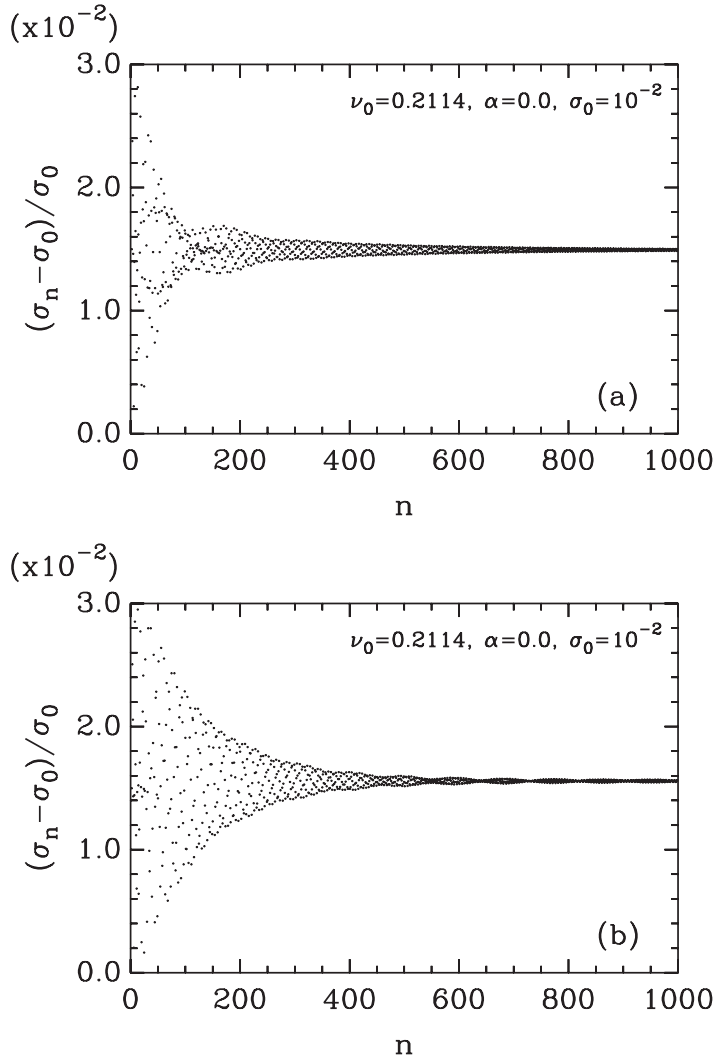


**Figure 1.** Evolution of the average action of the Hénon map with $\nu_0 = 0.2114$ calculated by (*a*) using the moment map (53) and (*b*) multi-particle simulations. The initial average action is $\sigma_0 = 10^{-2}$ and $n$ is the number of turns.

variables, it is understandable that the detail agreement between the moment map (53) and the direct tracking is not very good during the transient oscillation where the detail dynamics of the angular variables are important. In figure 2, the stationary average action is plotted as a function of $\nu_0$ where the ratio of octupole and sextupole strengths is $\alpha = \epsilon_2/\epsilon_1^2 = 2$. Qualitatively good agreement is found between the moment map and the direct tracking. Because of the sextupole and octupole perturbations, 1/2, 1/3, and 1/4 resonances are the dominant resonances and a strong growth of the average action occurs near these resonances. Near the 1/4 resonance, the increase of the average action calculated by using the moment map is about ten times larger than that by the direct tracking. This discrepancy could be due to high-order effects that are neglected in the moment map since high-order perturbations may stabilize low-order instabilities.

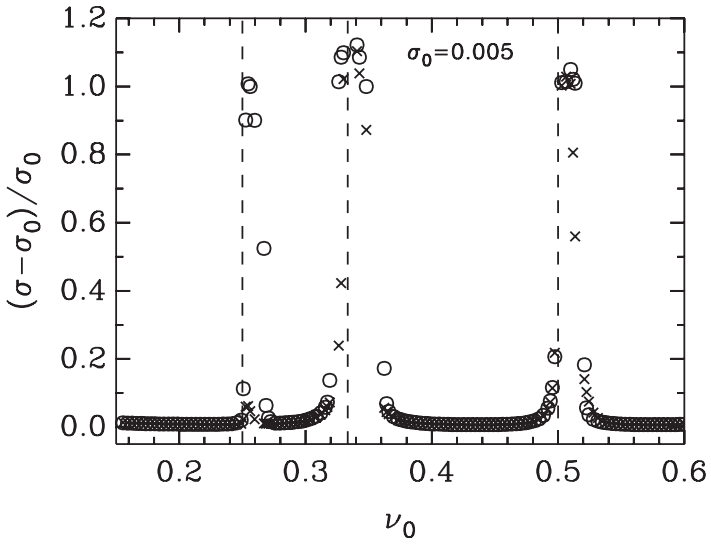


**Figure 2.** The increase of the stationary average action of map (49) with a sextupole and octupole as a function of $\nu_0$ calculated by using the moment map (53) (circle) and by the multi-particle tracking (cross). The initial average action $\sigma_0 = 5 \times 10^{-3}$ and $\alpha = 2$. The dashed lines indicate $\nu_0 = 1/2, 1/3$, and $1/4$. Due to the amplitude dependence of frequency, the location of the resonances are shifted.

It should be noted that the moment map derived from equation (49) is the result of a second-order perturbative calculation. It will fail when the system becomes globally chaotic, which generally occurs outside the dynamic aperture. When $\sigma_0$ is comparable to the dynamic aperture, the stationary state of the average action no longer exists due to rapid particle loss and the moment map diverges. On the other hand, when a particle beam is initially inside the dynamic aperture, the moment map qualitatively describes the growth of the beam size even when the system is very close to strong primary resonances, as shown in figure 2. For example, when $\nu_0 = 0.339$ and $\alpha = 2.0$, the system is dominated by strong 1/3 resonance as shown by the phase-space portrait of map (49) in figure 3. The dynamic aperture in this case is at $I = (x^2 + p^2)/2 \simeq 0.03$. For $\sigma_0 = 0.005$, the stationary average action calculated from the moment map is $(\sigma - \sigma_0)/\sigma_0 \simeq 1.0$ which agrees well with that from the multi-particle tracking (see figure 2) even though in this case particles at $3\sigma_0$ of the distribution are fairly close to the dynamic aperture. In this case, the strong growth of the average action is mainly due to particles moving along the invariant curves that wind around 1/3 resonance to large amplitude of phase space.

(2) Non-integrable system with two and a half degrees of freedom. In this case, the nonlinear coupling between the two degrees of freedom is of particular interest. Consider a four-dimensional symplectic map that models two-dimensional transverse motion of beam particles in a hadron storage ring with one nonlinear element that is otherwise linear,

$$\begin{aligned} x_{n+1} &= x_n \cos 2\pi\nu_{x0} + [p_{x,n} + K_x(x, y)] \sin 2\pi\nu_{x0} \\ p_{x,n+1} &= -x_n \sin 2\pi\nu_{x0} + [p_{x,n} + K_x(x, y)] \cos 2\pi\nu_{x0} \\ y_{n+1} &= y_n \cos 2\pi\nu_{y0} + [p_{y,n} + K_y(x, y)] \sin 2\pi\nu_{y0} \\ p_{y,n+1} &= -y_n \sin 2\pi\nu_{y0} + [p_{y,n} + K_y(x, y)] \cos 2\pi\nu_{y0} \end{aligned} \tag{56}$$

where $\nu_{x0}$ and $\nu_{y0}$ are the frequencies associated to the linear horizontal ($x$) and vertical ($y$)

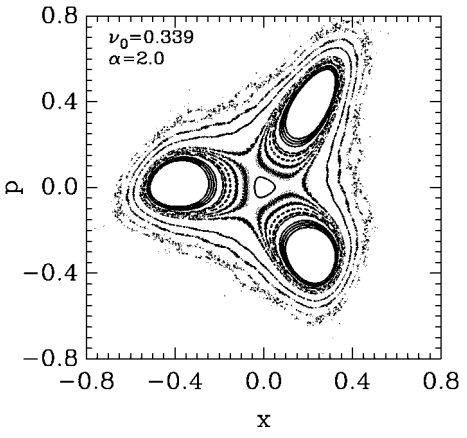


**Figure 3.** Phase-space portrait of map (49) with a sextupole and octupole. $\nu_0 = 0.339$ and $\alpha = 2.0$. The dynamic aperture is at $I = (x^2 + p^2)/2 \simeq 0.03$.

motions, respectively. The nonlinear kick is determined by the perturbative potential $H_1(x, y)$ through

$$K_x = -\frac{\partial H_1(x, y)}{\partial x} \qquad K_y = -\frac{\partial H_1(x, y)}{\partial y}. \tag{57}$$

The map is thus generated by the Hamiltonian

$$H = \nu_{x0} I_x + \nu_{y0} I_y + H_1\left(\sqrt{2I_x}\cos\phi_x, \sqrt{2I_y}\cos\phi_y\right) \delta_p(t). \tag{58}$$

We again consider only sextupole and octupole perturbations of which the perturbative Hamiltonian is

$$H_1 = -\frac{\epsilon_1}{3}(x^3 - 3xy^2) - \frac{\epsilon_2}{4}(x^4 + y^4 - 6x^2y^2). \tag{59}$$

With the action–angle variables, the Fourier components of $H_1$ can be easily obtained and the two-dimensional nonlinear map for the first-order moments $(\sigma_x, \sigma_y)$ can then be obtained from equation (48) as detailed in the appendix.

To examine the validity of the two-dimensional moment map in equations (A.21) and (A.22) of the appendix, the time evolution of the moments calculated by using the moment map is compared with the result of multi-particle simulations. Figures 4–7 plot the evolution of two nonlinear-coupled $\sigma_x$ and $\sigma_y$ for two different cases. In the case of figures 4 and 5, only sextupole perturbation is included ($\alpha = 0$) and the original map in equation (56) is the four-dimensional Hénon map. In the case of figures 6 and 7, both sextupole and octupole are included. In both situations and also in other cases with different parameters we studied, good agreement between the moment map and the direct simulation was found. Similar to the situation of one and a half degrees of freedom, when the initial moments $\sigma_{x,0}$ and $\sigma_{y,0}$ are not too big and $\vec{\nu}_0$ is not close to a major resonance, a stationary state for the average actions exists for all the cases we studied and we also found that the smaller the initial moments, the longer the transient. It should be noted that our previous approach [7] failed in this case.

(3) An isolated difference resonance in two and a half degrees of freedom. Resonances appear whenever $m_1\nu_{x0} + m_2\nu_{y0} = n$, where $m_1$, $m_2$ and $n$ are integers. When the system is close to a resonance that leads to strong instability, the perturbation formula in equation (44) is no longer appropriate for studying the growth of the first-order moments. On the other hand, in the system with two degrees of freedom and time dependence, an isolated difference resonance ($m_1m_2 < 0$) does not lead to an instability, i.e. the motion is always confined in both $x$ and $y$ directions [12,13]. The moments in two directions are therefore bounded. Due to the nonlinear

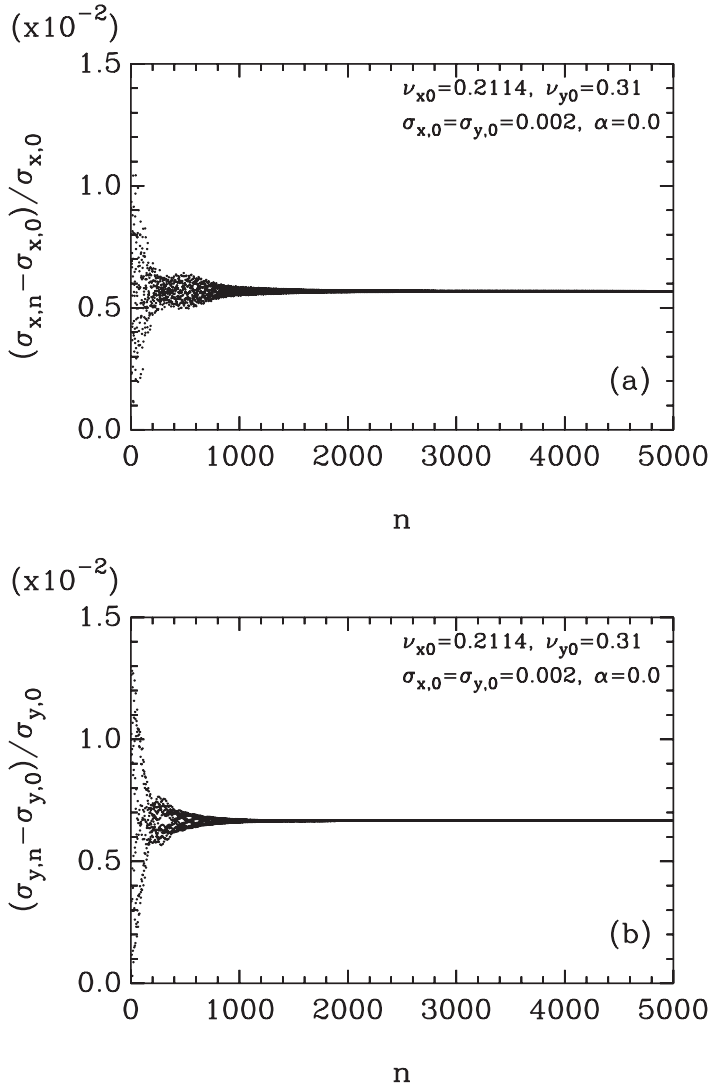


**Figure 4.** Evolution of two coupled average actions (*a*) in the $x$-direction and (*b*) in the $y$-direction of four-dimensional Hénon map calculated by using the moment map (A.21), (A.22). The linear frequency $\nu_{x0} = 0.2114$, $\nu_{y0} = 0.31$ and initial value $\sigma_{x,0} = \sigma_{y,0} = 2 \times 10^{-3}$.

coupling, however, the energy could be transferred from one direction to the other. As a result, an initially very small moment in one direction could grow to a large value [6, 14]. To explore the behaviour in the neighbourhood of such a resonance with the perturbation formula, in this section we study an isolated difference resonance of sextupole.

Suppose that a system is close to a difference resonance of the form $\nu_{x0} - 2\nu_{y0} = n$ and all other non-resonant terms in the Hamiltonian can be neglected. The perturbative Hamiltonian can thus be truncated as

$$H_1 = \frac{\epsilon_1}{4}(2I_x)^{1/2}(2I_y)\cos(\phi_x - 2\phi_y)\,\delta_p(t). \tag{60}$$

Since the Hamiltonian depends only on $\phi_x - 2\phi_y$ for angle variables, $2I_x + I_y$ is a constant of

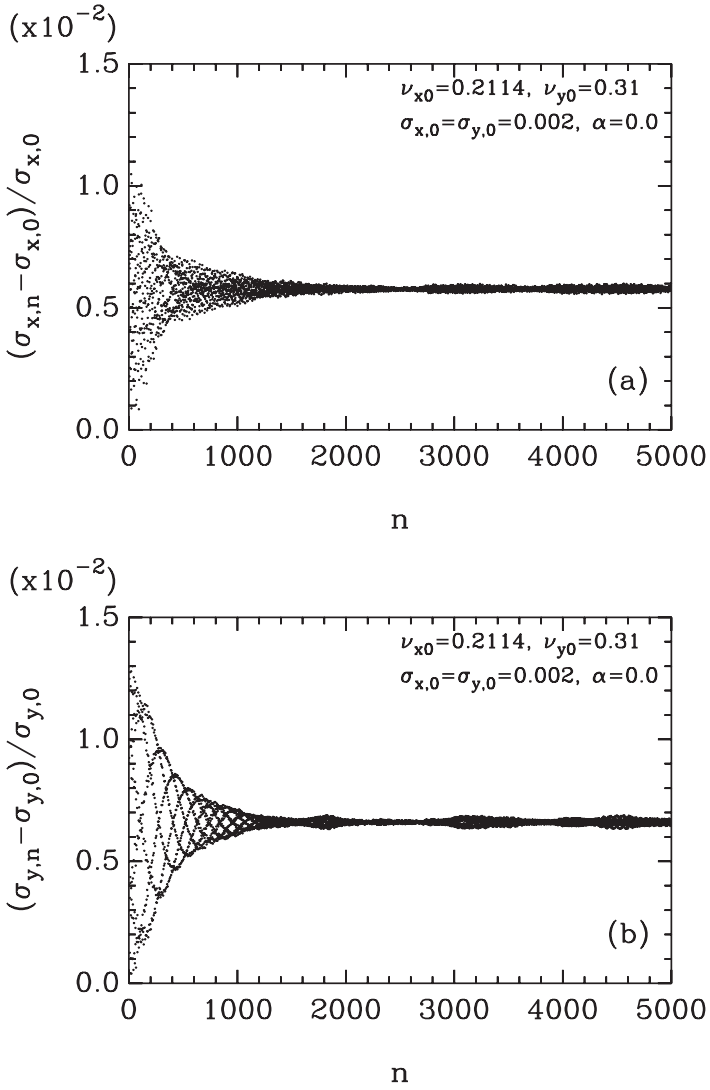


**Figure 5.** As figure 4 but calculated by the multi-particle tracking.

motion. Substituting equation (60) into (48) yields

$$\sigma_{x,n+1} = \sigma_{x,n} + A_n \qquad \sigma_{y,n+1} = \sigma_{y,n} - 2A_n \tag{61}$$

where

$$A_n = \sigma_{y,n}\left(\sigma_{y,n} - 2\sigma_{x,n}\right) + 2\sum_{m=1}^{n} \sigma_{y,n-m}\left(\sigma_{y,n-m} - 2\sigma_{x,n-m}\right) C_{mn} \tag{62}$$

$$C_{mn} = R_{12}\left(2\pi m \nu_{M0}, -\frac{m}{2}\cot(\pi\nu_{M0})\sigma_{x,n-m}, \frac{m}{2}\cot(\pi\nu_{M0})\sigma_{y,n-m}\right) \tag{63}$$

and $\nu_{M0} = \nu_{x0} - 2\nu_{y0}$. It follows that

$$2\sigma_{x,n} + \sigma_{y,n} = \text{constant} \tag{64}$$

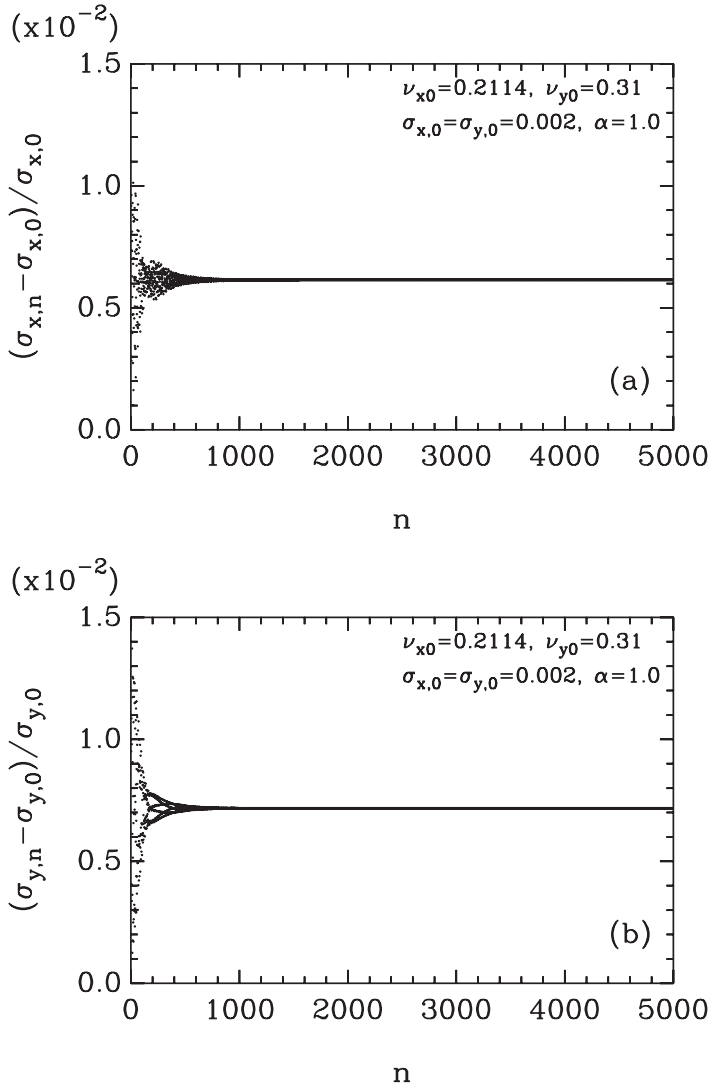


**Figure 6.** Evolution of two coupled average action (*a*) in the $x$-direction and (*b*) in the $y$-direction of the modified four-dimensional Hénon map with an additional octupole nonlinearity with $\alpha = 1.0$ calculated by using the moment map (A.21), (A.22). The other parameters are the same as those in figure 4.

which corresponds to the constant of motion of the system. Since both $\sigma_x$ and $\sigma_y$ are positively defined, they are bounded by equation (64). It should be noted, however, that for the approximated moment map to be valid the frequency shifts due to the amplitude dependence of the frequencies should be much smaller than the original frequencies. In this case it is necessary that $\frac{1}{2}|\cot(\pi\nu_{M0})|\ \max\left(\sigma_{x,0}, \sigma_{y,0}\right) \ll 2\pi\nu_{M0}$.

Figure 8 shows a typical case of evolution of $\sigma_x$ and $\sigma_y$ calculated from the moment map (61). The result is in very good agreement with the results from multi-particle simulation [6, 14]. In fact, the stationary average action can be directly obtained from the

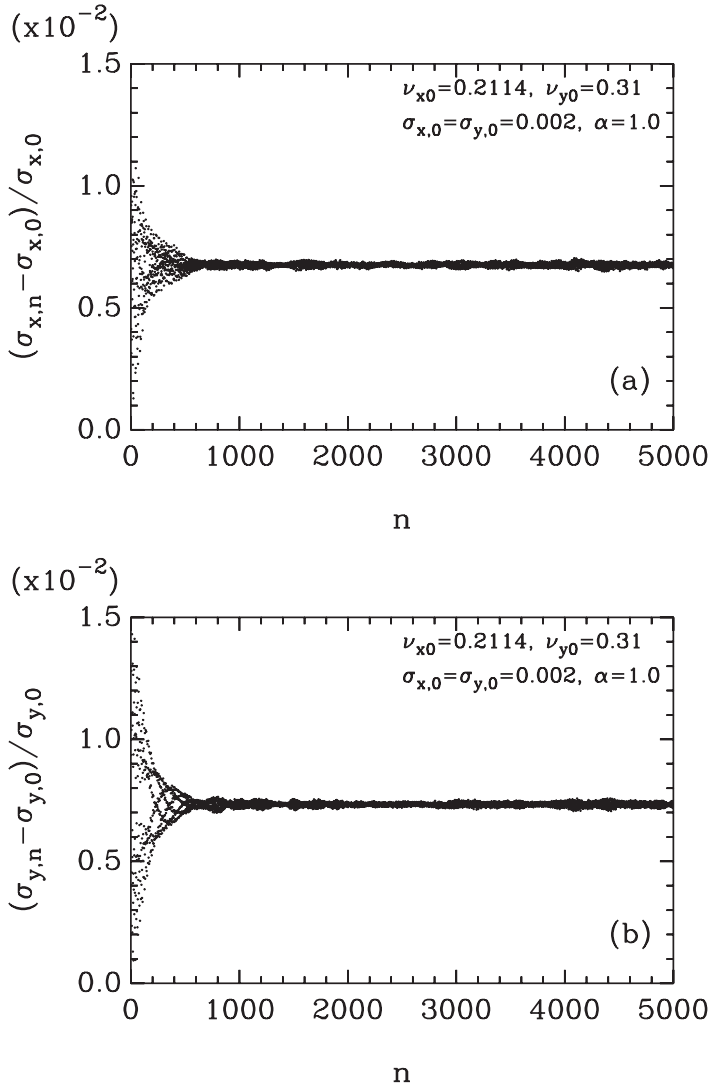


**Figure 7.** As figure 6 but calculated by the multi-particle tracking.

map (61). The fixed point of the map (61), $(\sigma_x, \sigma_y)$, which corresponds to the stationary state, is

$$\sigma_y - 2\sigma_x = 0. \tag{65}$$

Together with equation (64), the stationary state is found to be

$$\sigma_x = \tfrac{1}{4}\left(2\sigma_{x,0} + \sigma_{y,0}\right) \qquad \sigma_y = \tfrac{1}{2}\left(2\sigma_{x,0} + \sigma_{y,0}\right). \tag{66}$$

Near the resonance, this stationary state is locally stable [14]. It implies that for an initial Gaussian distribution with $\sigma_{x,0}$ and $\sigma_{y,0}$ not too far away from the stationary values, the final state of $(\sigma_x, \sigma_y)$ will achieve these stationary values.

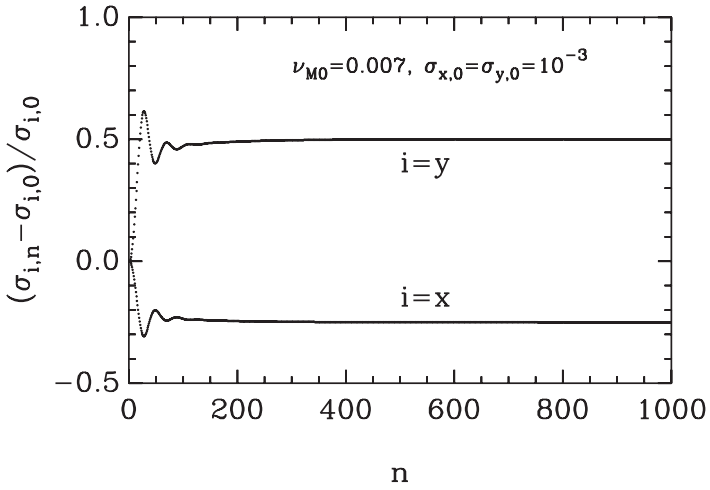


**Figure 8.** Evolution of two coupled average actions in a case of an isolated difference resonance calculated by using moment map (61). $\nu_{M0} = \nu_{x0} - 2\nu_{y0} = 0.007$ and $\sigma_{x,0} = \sigma_{y,0} = 10^{-3}$.

## 6. Summary

Using the method of projection operator, we have derived from the Liouville equation the evolution equation of the angle-averaged distribution function in action space for weakly non-integrable Hamiltonian systems such as beam particles in hadron storage rings. For the kick-type perturbations such as beam–beam interactions or localized magnetic field errors in particle storage rings, this treatment results in a functional map for the angle-averaged distribution function. With the Gaussian distribution approximation, this functional map can be reduced to a moment map which can easily be iterated numerically for studying the evolution of the moments. To test this method, the evolution of the averaged action variables is studied on systems with one and a half as well as two and a half degrees of freedom. The averaged action variables calculated by using the angle-averaged distribution function was compared with that of multi-particle simulations. The comparison study with various values of system parameters showed that the angle-averaged distribution function provides a valid description of the evolution of the averaged action variables except when the system is close to major resonances. When the system is close to major resonances, the particle distribution in phase space may deviate too quickly and too far from its initial distribution to be considered within the framework of the method of projection operator. Large particle storage rings, however, are generally operated far from all major resonances and the angle-averaged distribution function is an effective means for studying the beam-size growth due to weak nonlinear perturbations.

## Acknowledgments

This work was supported by the US Department of Energy under Grant No. DE-FG03-00ER41153 and the University of Kansas General Research Fund. We would also like to thank the Center for Advanced Scientific Computing at the University of Kansas for the use of the supercomputer. DY is on leave from Center for Fundamental Physics, University of Science and Technology of China. He acknowledges support from China National Natural Science Foundation.

## Appendix. First-order-moment map for four-dimensional symplectic map

In this appendix, the nonlinear map for the first-order moments are obtained for the four-dimensional symplectic map given by equations (56)–(59) in section 5.2. The nonzero Fourier components of $H_1$ in equation (59), in the form of (35), are

$$h_{0,0} = -\frac{3\epsilon_2}{8}\left(I_x^2 + I_y^2 - 4I_x I_y\right) \tag{A.1}$$

$$h_{1,0} = h_{-1,0} = -\frac{\epsilon_1}{2\sqrt{2}}\left(I_x^{3/2} - 2I_x^{1/2} I_y\right) \tag{A.2}$$

$$h_{1,2} = h_{1,-2} = h_{-1,2} = h_{-1,-2} = \frac{\epsilon_1}{2\sqrt{2}} I_x^{1/2} I_y \tag{A.3}$$

$$h_{2,0} = h_{-2,0} = -\frac{\epsilon_2}{4}\left(I_x^2 - 3I_x I_y\right) \tag{A.4}$$

$$h_{2,2} = h_{-2,-2} = h_{2,-2} = h_{-2,2} = \frac{3\epsilon_2}{8} I_x I_y \tag{A.5}$$

$$h_{0,2} = h_{0,-2} = -\frac{\epsilon_2}{4}\left(I_y^2 - 3I_x I_y\right) \tag{A.6}$$

$$h_{3,0} = h_{-3,0} = -\frac{\epsilon_1}{6\sqrt{2}} I_x^{3/2} \tag{A.7}$$

$$h_{4,0} = h_{-4,0} = -\frac{\epsilon_2}{16} I_x^2 \tag{A.8}$$

$$h_{0,4} = h_{0,-4} = -\frac{\epsilon_2}{16} I_y^2. \tag{A.9}$$

The frequencies of the nonlinear motion of the four-dimensional map, including the amplitude dependence, can be calculated from equation (45) as

$$\nu_x = \nu_{x0} + \frac{\epsilon_1^2}{2\pi}\left(\lambda_{xx} I_x + \lambda_{xy} I_y\right) \tag{A.10}$$

$$\nu_y = \nu_{y0} + \frac{\epsilon_1^2}{2\pi}\left(\lambda_{xy} I_x + \lambda_{yy} I_y\right) \tag{A.11}$$

where

$$\lambda_{xx} = -\tfrac{1}{8}[3\cot(\pi\nu_{x0}) + \cot(3\pi\nu_{x0}) + 6\alpha] \tag{A.12}$$

$$\lambda_{xy} = -\tfrac{1}{4}\left\{\cot[\pi(\nu_{x0} + 2\nu_{y0})] - \cot[\pi(\nu_{x0} - 2\nu_{y0})] - 2\cot(\pi\nu_{x0}) - 6\alpha\right\} \tag{A.13}$$

$$\lambda_{yy} = -\tfrac{1}{8}\left\{\cot[\pi(\nu_{x0} + 2\nu_{y0})] + \cot[\pi(\nu_{x0} - 2\nu_{y0})] + 6\alpha\right\}. \tag{A.14}$$

In calculating the amplitude dependence of frequencies, we again include only the first-order contribution from octupole and the second-order contribution from sextupole. To simplify the notation, let

$$\nu_{P0} = \nu_{x0} + 2\nu_{y0} \qquad \nu_{M0} = \nu_{x0} - 2\nu_{y0} \tag{A.15}$$

$$\lambda_{Px} = \lambda_{xx} + 2\lambda_{xy} \qquad \lambda_{Py} = \lambda_{xy} + 2\lambda_{yy} \tag{A.16}$$

$$\lambda_{Mx} = \lambda_{xx} - 2\lambda_{xy} \qquad \lambda_{My} = \lambda_{xy} - 2\lambda_{yy} \tag{A.17}$$

$$\nu_{+0} = \nu_{x0} + \nu_{y0} \qquad \nu_{-0} = \nu_{x0} - \nu_{y0} \tag{A.18}$$

$$\lambda_{+x} = \lambda_{xx} + \lambda_{xy} \qquad \lambda_{+y} = \lambda_{xy} + \lambda_{yy} \tag{A.19}$$

$$\lambda_{-x} = \lambda_{xx} - \lambda_{xy} \qquad \lambda_{-y} = \lambda_{xy} - \lambda_{yy}. \tag{A.20}$$

The nonlinear map for the first-order moments can then be obtained from equation (48) as

$$\sigma_{x,n+1} = \sigma_{x,n} + \tfrac{1}{2}\left[\left(3\sigma_{x,n}^2 - 2\sigma_{x,n}\sigma_{y,n} + 3\sigma_{y,n}^2\right) + 3\alpha^2\left(5\sigma_{x,n}^3 - 6\sigma_{x,n}^2\sigma_{y,n} + 9\sigma_{x,n}\sigma_{y,n}^2\right)\right]$$

$$
\begin{aligned}
&+\tfrac{1}{2}\sum_{m=1}^{n}\{3\sigma_{x,n-m}^{2}\big[R_{30}\left(2\pi m\nu_{x0}, m\lambda_{xx}\sigma_{x,n-m}, m\lambda_{xy}\sigma_{y,n-m}\right)\\
&+R_{30}\left(6\pi m\nu_{x0}, 3m\lambda_{xx}\sigma_{x,n-m}, 3m\lambda_{xy}\sigma_{y,n-m}\right)\big]\\
&-2\sigma_{x,n-m}\sigma_{y,n-m}\big[2R_{12}\left(2\pi m\nu_{x0}, m\lambda_{xy}\sigma_{y,n-m}, m\lambda_{xx}\sigma_{x,n-m}\right)\\
&-R_{12}\left(2\pi m\nu_{P0}, m\lambda_{Px}\sigma_{x,n-m}, m\lambda_{Py}\sigma_{y,n-m}\right)\\
&+R_{12}\left(2\pi m\nu_{M0}, m\lambda_{Mx}\sigma_{x,n-m}, m\lambda_{My}\sigma_{y,n-m}\right)\big]\\
&+\sigma_{y,n-m}^{2}\big[4R_{12}\left(2\pi m\nu_{x0}, m\lambda_{xx}\sigma_{x,n-m}, m\lambda_{xy}\sigma_{y,n-m}\right)\\
&+R_{12}\left(2\pi m\nu_{P0}, m\lambda_{Px}\sigma_{x,n-m}, m\lambda_{Py}\sigma_{y,n-m}\right)\\
&+R_{12}\left(2\pi m\nu_{M0}, m\lambda_{Mx}\sigma_{x,n-m}, m\lambda_{My}\sigma_{y,n-m}\right)\big]\\
&+6\alpha^{2}\sigma_{x,n-m}^{3}\big[4R_{40}\left(4\pi m\nu_{x0}, 2m\lambda_{xx}\alpha\sigma_{x,n-m}, 2m\lambda_{xy}\alpha\sigma_{y,n-m}\right)\\
&+R_{40}\left(8\pi m\nu_{x0}, 4m\lambda_{xx}\alpha\sigma_{x,n-m}, 4m\lambda_{xy}\alpha\sigma_{y,n-m}\right)\big]\\
&-9\alpha^{2}\sigma_{x,n-m}^{2}\sigma_{y,n-m}\big[4R_{31}\left(4\pi m\nu_{x0}, 2m\lambda_{xx}\alpha\sigma_{x,n-m}, 2m\lambda_{xy}\alpha\sigma_{y,n-m}\right)\\
&-R_{22}\left(4\pi m\nu_{+0}, 2m\lambda_{+x}\alpha\sigma_{x,n-m}, 2m\lambda_{+y}\alpha\sigma_{y,n-m}\right)\\
&+R_{22}\left(4\pi m\nu_{-0}, 2m\lambda_{-x}\alpha\sigma_{x,n-m}, 2m\lambda_{-y}\alpha\sigma_{y,n-m}\right)\big]\\
&+9\alpha^{2}\sigma_{x,n-m}\sigma_{y,n-m}^{2}\big[4R_{22}\left(4\pi m\nu_{x0}, 2m\lambda_{xx}\alpha\sigma_{x,n-m}, 2m\lambda_{xy}\alpha\sigma_{y,n-m}\right)\\
&+R_{22}\left(4\pi m\nu_{+0}, 2m\lambda_{+x}\alpha\sigma_{x,n-m}, 2m\lambda_{+y}\alpha\sigma_{y,n-m}\right)\\
&+R_{22}\left(4\pi m\nu_{-0}, 2m\lambda_{-x}\alpha\sigma_{x,n-m}, 2m\lambda_{-y}\alpha\sigma_{y,n-m}\right)\big]\}
\end{aligned}
\tag{A.21}
$$

$$
\begin{aligned}
\sigma_{y,n+1} = \sigma_{y,n} + \Big[&2\sigma_{x,n}\sigma_{y,n} + \frac{3\alpha^{2}}{2}\left(5\sigma_{y,n}^{3} - 6\sigma_{y,n}^{2}\sigma_{x,n} + 9\sigma_{y,n}\sigma_{x,n}^{2}\right)\Big]\\
&+\tfrac{1}{2}\sum_{m=1}^{n}\{4\sigma_{x,n-m}\sigma_{y,n-m}\big[R_{12}\left(2\pi m\nu_{P0}, m\lambda_{Px}\sigma_{x,n-m}, m\lambda_{Py}\sigma_{y,n-m}\right)\\
&+R_{12}\left(2\pi m\nu_{M0}, m\lambda_{Mx}\sigma_{x,n-m}, m\lambda_{My}\sigma_{y,n-m}\right)\big]\\
&+2\sigma_{y,n-m}^{2}\big[R_{12}\left(2\pi m\nu_{P0}, m\lambda_{Px}\sigma_{x,n-m}, m\lambda_{Py}\sigma_{y,n-m}\right)\\
&-R_{12}\left(2\pi m\nu_{M0}, m\lambda_{Mx}\sigma_{x,n-m}, m\lambda_{My}\sigma_{y,n-m}\right)\big]\\
&+6\alpha^{2}\sigma_{y,n-m}^{3}\big[4R_{40}\left(4\pi m\nu_{y0}, 2m\lambda_{yy}\alpha\sigma_{y,n-m}, 2m\lambda_{xy}\alpha\sigma_{x,n-m}\right)\\
&+R_{40}\left(8\pi m\nu_{y0}, 4m\lambda_{yy}\alpha\sigma_{y,n-m}, 4m\lambda_{xy}\alpha\sigma_{x,n-m}\right)\big]\\
&-9\alpha^{2}\sigma_{y,n-m}^{2}\sigma_{x,n-m}\big[4R_{31}\left(4\pi m\nu_{y0}, 2m\lambda_{yy}\alpha\sigma_{y,n-m}, 2m\lambda_{xy}\alpha\sigma_{x,n-m}\right)\\
&-R_{22}\left(4\pi m\nu_{+0}, 2m\lambda_{+y}\alpha\sigma_{y,n-m}, 2m\lambda_{+x}\alpha\sigma_{x,n-m}\right)\\
&+R_{22}\left(-4\pi m\nu_{-0}, -2m\lambda_{-y}\alpha\sigma_{y,n-m}, -2m\lambda_{-x}\alpha\sigma_{x,n-m}\right)\big]\\
&+9\alpha^{2}\sigma_{y,n-m}\sigma_{x,n-m}^{2}\big[4R_{22}\left(4\pi m\nu_{y0}, 2m\lambda_{yy}\alpha\sigma_{y,n-m}, 2m\lambda_{xy}\alpha\sigma_{x,n-m}\right)\\
&+R_{22}\left(4\pi m\nu_{+0}, 2m\lambda_{+y}\alpha\sigma_{y,n-m}, 2m\lambda_{+x}\alpha\sigma_{x,n-m}\right)\\
&+R_{22}\left(-4\pi m\nu_{-0}, -2m\lambda_{-y}\alpha\sigma_{y,n-m}, -2m\lambda_{-x}\alpha\sigma_{x,n-m}\right)\big]\}
\end{aligned}
\tag{A.22}
$$

where $\sigma_{x,n} = \epsilon_1^2 M_{xn}$, $\sigma_{y,n} = \epsilon_1^2 M_{yn}$ and

$$
\begin{aligned}
R_{30}(x, y, z) = \frac{1}{(1+y^2)^4(1+z^2)}\big\{&\left[(1-6y^2+y^4) - 4yz(1-y^2)\right]\cos x\\
&-\left[4y(1-y^2) + z(1-6y^2+y^4)\right]\sin x\big\}
\end{aligned}
\tag{A.23}
$$

$$
R_{12}(x, y, z) = \frac{1}{(1+y^2)^2(1+z^2)^3}\big\{\left[(1-y^2)(1-3z^2) - 2yz(3-z^2)\right]\cos x
$$

$$-\left[2y(1-3z^2)+z(1-y^2)(3-z^2)\right]\sin x\Big\} \tag{A.24}$$

$$R_{40}(x,y,z)=\frac{1}{(1+y^2)^5(1+z^2)}\Big\{\left[(1-10y^2+5y^4)-yz(5-10y^2+y^4)\right]\cos x$$
$$-\left[y(5-10y^2+y^4)+z(1-10y^2+5y^4)\right]\sin x\Big\} \tag{A.25}$$

$$R_{31}(x,y,z)=\frac{1}{(1+y^2)^4(1+z^2)^2}\Big\{\left[(1-6y^2+y^4)(1-z^2)-8yz(1-y^2)\right]\cos x$$
$$-\left[4y(1-y^2)(1-z^2)+2z(1-6y^2+y^4)\right]\sin x\Big\} \tag{A.26}$$

$$R_{22}(x,y,z)=\frac{1}{(1+y^2)^3(1+z^2)^3}\Big\{\left[(1-3y^2)(1-3z^2)-yz(3-y^2)(3-z^2)\right]\cos x$$
$$-\left[y(3-y^2)(1-3z^2)+z(1-3y^2)(3-z^2)\right]\sin x\Big\}. \tag{A.27}$$

Note the symmetries $R_{22}(x,y,z)=R_{22}(x,z,y)$ and $R_{22}(x,y,z)=R_{22}(-x,-z,-y)$. Therefore, each of the $R_{22}$ in equation (A.22) has the same value as the corresponding one in equation (A.21). It should also be noted that when $\sigma_{y,0}=0$, equation (53) is recovered.

## References


[1] Zaslavsky G M 1985 *Chaos in Dynamical Systems* (New York: Harwood) chapter 6

[2] Sagdeev R Z, Usikov D A and Zaslavsky G M 1988 *Nonlinear Physics* (New York: Harwood) chapter 6

[3] Lichtenberg A J and Liberman M A 1992 *Regular and Chaotic Dynamics* 2nd edn (New York: Springer) chapter 5

[4] Bazzani A, Siboni S and Turchetti G 1994 Diffusion in Hamiltonian systems with a small stochastic perturbation *Physica* D **76** 8

[5] Bazzani A and Turchetti G 1997 Action diffusion for symplectic maps with a noisy linear frequency *J. Phys. A: Math. Gen.* **30** 27

[6] Shi J and Ohnuma S 1993 Perturbation expansion for particle distributions in hadron storage rings *Phys. Rev.* E **47** 4405

[7] Yao D and Shi J 1998 Method of projection operator for the study of angle-averaged distribution function of beam particles in hadron storage rings *Phys. Rev.* SP-AB **1** 084001

[8] Grabert H 1982 *Projection Operator Techniques in Nonequilibrium Statistical Mechanics* (New York: Springer) chapter 2

[9] Tzenov S I 1995 *Long Term Behavior in Multi-Dimensional Hamiltonian Systems (Nonlinear Diffusion Approach) (AIP Conf. Proc.* vol 344) (New York: AIP) p 259

[10] Channell P J 1999 Systematic solution of the Vlasov-poisson equations for charged particle beams *Phys. Plasma* **6** 982

[11] Bazzani A, Mazzanti P, Servizi S and Turchetti G 1988 Normal forms for Hamiltonian maps and nonlinear effects in a particle accelerator Il *Nucl. Phys.* B **102** 51

[12] Sturrock P A 1958 *Ann. Phys., NY* **3** 113

[13] Ohnuma S and Gluckstern R L 1985 *IEEE Trans. Nucl. Sci.* **NS-32** 2261

[14] Shi J, Huang Y and Ohnuma S 1991 Phase-space distribution of particles near an isolated difference resonance *Proc. IEEE 1991 Particle Accelerator Conf.* (New York: IEEE) p 407